2008 International Symposium on Nonlinear Theory and its Applications
NOLTA'08, Budapest, Hungary, September 7-10, 2008

An MC-UWB system with overlapping Gaussian subcarriers

Yutaka Jitsumatsu and Tohru Kohda

Dept. of Computer Science and Communication Engineerings, Kyushu University
744 Motooka, Nishi-ku, Fukuoka, 819-0395, Japan
E-mail: {jitumatu, kohda}@csce.kyushu-u.ac.jp

Abstract—It was recently shown that chaos-based spreading codes generated by a Markov map improve the bit rate of direct sequence ultra wideband (DS-UWB) impulse radio systems. In order to enhance the spectral efficiency, we propose a multi-carrier UWB system with Gaussian-shaped subcarriers, where interferences between quasi-orthogonal subcarriers are mitigated by Markov codes.

1. Introduction

One of the significant findings in chaos-based spread-spectrum (SS) communication is that spreading codes generated from a Markov chain outperform the conventional linear-feedback shift register sequences in asynchronous code division multiple access (CDMA) systems [1, 2]. The superiority of Markovian codes in SS communications has been established by G. Setti, R. Rovatti, and G. Mazzini. See [3] and references therein. Joint optimization of pulse shaping filter and spreading codes are discussed in [4]. A Markov chain can be embedded into a one-dimensional piecewise-linear map [5].

Recent communication systems based on SS techniques include multicarrier CDMA and ultra wideband (UWB) communications. The above research group showed that Markov codes are promising in such advanced systems, too. The peak-to-average power ratio (PAPR) of multi-carrier DS-CDMA system can be improved by Markov codes [6]. Recently, it was shown that Markov codes improve the data transmission rate of DS-UWB sensor networks up to 20% [7, 8].

The UWB communications have attracted an enormous attention because we can use a huge bandwidth (a frequency band from 3.1GHz to 10.6GHz) with very small low power density, overlaying coexistent RF systems. In the UWB communications, a sequence of impulses whose pulse durations are less than one nano-second is used as an information bearer. Its expected applications include wireless personal area networks (WPAN), sensor networks, imaging systems, and vehicular radar systems [9].

Gaussian and Gaussian monocycle pulses were regarded as good candidates for UWB impulse. These Gaussian pulses are readily available from the antenna pattern[9]. However, Gaussian pulses exhibit a poor fit to the spectral mask of the Federal Communications Commission (FCC) [10, 11]. The spectral density of power emission from transmit antenna is strictly restricted to extremely low level, therefore pulse design is rather crucial in UWB communications than in other conventional systems.

Orthogonal frequency division multiplex (OFDM) systems are expected to enhance the spectral efficiency. However the orthogonality of subcarriers will be easily corrupted by timing and frequency synchronization errors. Such a situation motivated us to consider non-orthogonal (*quasi-orthogonal*) multicarrier UWB systems. We employ Gaussian-shaped subcarriers overlapping each other. Gaussian subcarriers are not orthogonal and thus cause inter-carrier interference (ICI). However the effect of ICI can be mitigated by Markov codes. For simplicity, we assume perfect synchronization, but the proposed quasi-orthogonal system can also be used in asynchronous environment.

2. UWB Impulse design

The FCC spectral masks for indoor and outdoor communications are illustrated in Fig 1. Let us define $W_1 = 0.96$, $W_2 = 1.61$, $W_3 = 1.99$, $W_4 = 3.1$, and $W_5 = 10.6$ GHz. Note that an optimal UWB waveform is intuitively given by the inverse Fourier transform of this spectral mask, which is a linear combination of ideal sinc functions with frequencies W_1 to W_5. However, such a waveform is physically unrealizable.

The maximum rate of information transmission of continuous-time bandlimited Gaussian channel is characterized by Shannon's celebrated capacity formula $C = W\log(1+\frac{P}{N_0 W})$, where W is the bandwidth, P is the received signal power and $N_0/2$ is the two-sided power spectral density of white Gaussian noise. In Shannon's original proof, an ideal filter, which is physically unrealizable, is assumed to achieve the capacity. Wyner [13] showed that Shannon's capacity of bandlimited Gaussian channel is actually achievable by physically realizable waveforms, i.e. prolate spheroidal wave functions (PSWFs) [14]. Slepian [15] rigorously proved a folk theorem: "the space of signals approximately bandlimited to W and approximately time-limited to T is $2WT$ dimensional," using PSWFs.

Parr et. al [10] proposed a digital FIR filter design, which is based on the PSWF. They used 3.1 to 10.6 GHz frequency band to define an integral equation

$$\gamma\phi(t) = \int_{-T/2}^{T/2} K(t,s)\phi(s)ds, \tag{1}$$

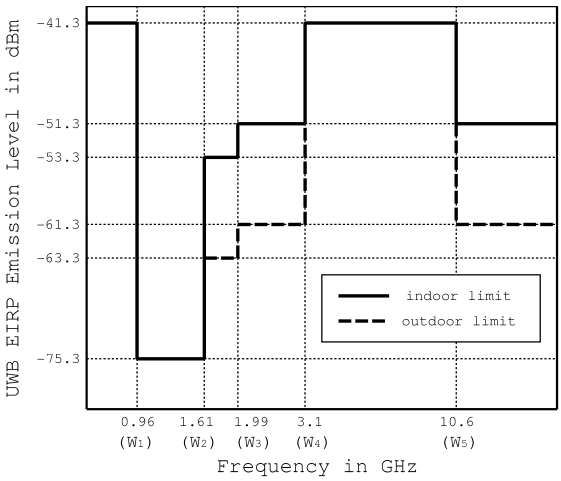

Figure 1: UWB spectral masks for indoor (solid line) and outdoor (dashed line) communication systems [9, 12]. EIRP implies equivalent isotropically radiated power and dBm is milliwatt in decibel.

with bandpass kernel

$$K(t,s) = \frac{\sin \pi(W_5 - W_4)(t-s)}{\pi(t-s)} \cos 2\pi f_c(t-s), \quad (2)$$

where $f_c = (W_5 + W_4)/2$ and $T = 1.0$ nano-second. In [10], the bandpass kernel is discretized to obtain a matrix eigenvalue problem at the sampling rate of 64GHz. Let $1 > \gamma_0 > \gamma_1 > \gamma_2 \ldots > 0$ be eigenvalues of the integral equation (1) and (2), where the eigenvalue γ_i expresses the inband energy

$$\beta^2 = \frac{\int_{W_4}^{W_5} |\tilde{\phi}(f)|^2 df + \int_{-W_5}^{-W_4} |\tilde{\phi}(f)|^2 df}{\int_{-\infty}^{\infty} |\tilde{\phi}(f)|^2 df}. \quad (3)$$

Two eigenvectors corresponding to the largest two eigenvalues are employed as orthogonal UWB impulses [10].

Remark 1: The first and second dominant eigenvectors are observed well approximated by

$$\hat{\phi}^{(0)}(t) \simeq \exp\left(\frac{-t^2}{2\sigma_\phi^2}\right)\cos(2\pi f_c t), \quad (4)$$

$$\hat{\phi}^{(1)}(t) \simeq \exp\left(\frac{-t^2}{2\sigma_\phi^2}\right)\sin(2\pi f_c t), \quad (5)$$

where $\sigma_\phi^2 = T/(2\pi)/(W_5 - W_4)$ is the variance of Gaussian envelope and $f_c = (W_5 + W_4)/2 = 6.85$ GHz is the center frequency. In Figs. 2 and 3, the two dominant eigenvectors at 64GHz and their approximation (4),(5) are plotted. We can choose **a)** using FIR filter with very high frequency 64GHz, which does not need carrier modulation or **b)** using FIR filter with relatively low frequency (the bandwidth 7.5GHz times up-sampling rate) together with carrier modulation at frequency $f_c = 6.85$GHz. The selection depends on manufacturing cost.

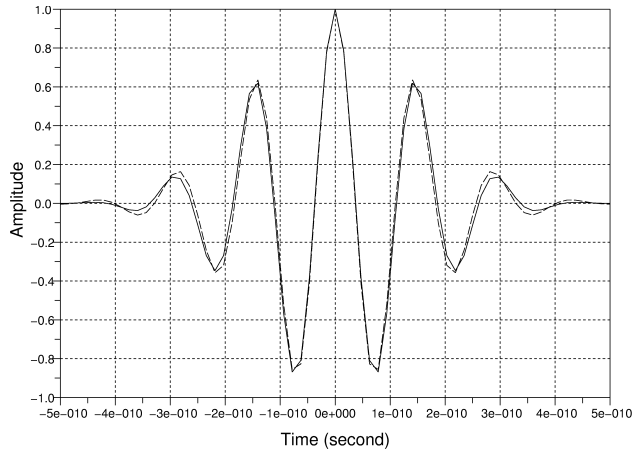

Figure 2: The first dominant eigenvector (solid curve) and Gaussian envelope with cosine wave (dashed curve).

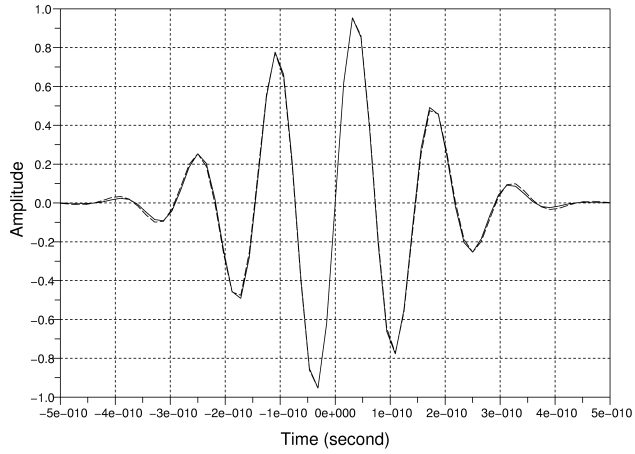

Figure 3: The second dominant eigenvector (solid curve) and Gaussian envelope with sine wave (dashed curve).

Note that the integral equation with bandpass kernel has no solution except for the case of degeneracy [16]. It might be better to employ **b)** for avoiding such a problem.

Remark 2: Parr et. al used only two eigenvectors, which however utilize the space of signals inefficiently. According to the 2WT theorem [15] and Wyner's result [13], using $2(W_5 - W_4)T - \varepsilon = 15 - \varepsilon$ eigenvectors gives optimal spectral efficiency, where ε is a small positive number. The frequency spectrum of the eigenvectors must satisfy the FCC spectral mask. The eigenvalues of Eqs.(1), (2) are listed in Table 1. Using 12 eigenvectors as orthogonal UWB impulses achieves the average inband energy 99.63% in the frequency band $[W_4, W_5]$.

A UWB waveform design based on Parks-McClellan algorithm is proposed in [17] and its improved version is proposed in [11], where waveform optimization is translated into a convex optimization problem and a pulse design for multi-band UWB systems and orthogonal UWB pulse design are also given. In [11], the sampling rate of finite im-

Table 1: List of eigenvalues of the passband kernel for [3.1, 10.6]GHz.

i	γ_i	i	γ_i
0	$1 - 3.0 * 10^{-10}$	8	0.9989804
1	$1 - 8.1 * 10^{-10}$	9	0.9977678
2	$1 - 4.1 * 10^{-8}$	10	0.9874811
3	$1 - 6.8 * 10^{-8}$	11	0.9720785
4	0.9999974	12	0.8972178
5	0.9999972	13	0.8159323
6	0.9999389	14	0.5666734
7	0.9998973	15	0.4361284

pulse response (FIR) filter is 28GHz. Note that this sampling rate causes an aliasing at 14GHz. A spectral margin between 10.6GHz and 14GHz might be insufficient.

We have so far discussed the pulse design satisfying FCC spectral mask, based on PSWFs. We showed that using twelve eigenvectors improves the rate of data transmission six times of [10]. We hereafter consider another method to improve the spectral efficiency, i.e. multi-carrier modulation with overlapping sub-carriers. In the next section, we discuss multicarrier modulation.

3. UWB multiple access system

A major scheme of UWB communication is impulse radio [18], where pulse position modulation (PPM) is used for data modulation, and pseudorandom time-hopping (TH) pattern is used to realize multiple access. The TH-PPM-UWB has advantage that its implementation is easy. On the other hand, the DS-UWB [19] and multi-band (MB)-OFDM [12] are the two strong candidates for WPAN communication standard. In OFDM systems, pulse shaping filter must satisfy an orthogonality condition. On the other hand, this paper considers multicarrier UWB systems with non-orthogonal (or, quasi-orthogonal) Gaussian subcarriers. Gaussian subcarriers cause inter-chip and inter-symbol interferences but their effects can be mitigated by Markov spreading codes.

Let $\phi_n(t)$ be a complex representation of a Gaussian waveform of n-th subcarrier, i.e.

$$\phi_n(t) = \exp\left(\frac{-t^2}{2\tau^2}\right) e^{-2\pi \mathrm{i} f_n t}, \tag{6}$$

where τ^2 is the variance of a Gaussian waveform, $\mathrm{i} = \sqrt{-1}$, and f_n is the frequency of n-th subcarrier. In Fig. 4, subcarriers with Gaussian waveform are illustrated, which are overlapping in frequency domain. According to the FCC mask (Fig. 1), W_p is determined by -10dB bandwidth and -20dB bandwidth for indoor and outdoor communications, respectively. The total bandwidth of an N subcarrier system is

$$W_{tot} = (N-1)\Delta f + W_p, \tag{7}$$

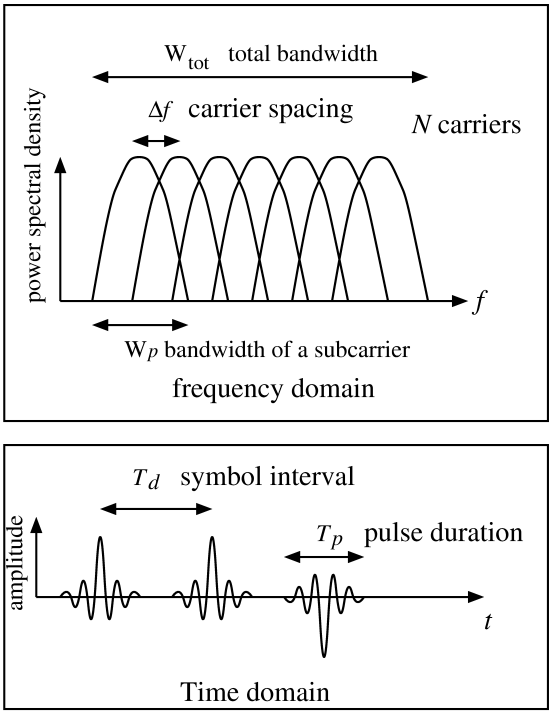

Figure 4: Sub-channels of multi-carrier modulation with Gaussian shaping.

where Δf is a carrier spacing. We refer to $W_p/\Delta f$ as packing ratio (PR), expressing the number of overlapping subcarriers in one bandwidth of the carrier.

The received signal is given by

$$r(t) = \sum_{k=1}^{K} \sum_{p=0}^{P-1} \sum_{n=0}^{N-1} d_p^{(k)} x_n^{(k)} \phi_n(t - pT_d) + n(t), \tag{8}$$

where K, P, N, and T_d are the number of users, the number of data symbols, a spreading factor, and the symbol duration. $d_p^{(k)}$, $x_n^{(k)}$, and $n(t)$ denote data symbol, spreading code, and additive white Gaussian noise with two-sided spectral density $N_0/2$, respectively.

We assume a single-user correlation receiver. The output of the k-th user's receiver of p-th period is

$$Z_p^{(k)} = \sum_{n=0}^{N-1} \overline{x_n^{(k)}} \int r(t) \overline{\phi_n(t - pT_d)} dt \tag{9}$$

$$= S_p^{(k)} + \mathrm{ISI}_p^{(k)} + \mathrm{MAI}_p^{(k)} + \eta_p^{(k)}, \tag{10}$$

where $\bar{z}$ is the complex conjugate of z, and S, ISI, MAI, and η denote, the signal component, inter-symbol interference, multiple-access interference and additive noise component. They are given by

$$S_p^{(k)} = d_p^{(k)} R_{MC}^{(k,k)}(p, p), \tag{11}$$

$$\mathrm{ISI}_p^{(k)} = \sum_{q \neq p} d_q^{(k)} R_{MC}^{(k,k)}(q, p), \tag{12}$$

$$\mathrm{MAI}_p^{(k)} = \sum_{j\neq k}\sum_{q=0}^{P-1} d_q^{(j)} R_{MC}^{(j,k)}(q,p), \tag{13}$$

where $R_{MC}^{(j,k)}(q,p) = \sum_{n=0}^{N-1}\sum_{m=0}^{N-1} \overline{x_n^{(k)}} x_m^{(j)} \int \overline{\phi_n(t-pT_d)}\phi_m(t-qT_d)dt$. Bit error rate is estimated by

$$P_e = Q\left(\sqrt{\mathrm{SINR}}\right), \qquad \mathrm{SINR} = (\mathrm{SIR}^{-1} + \frac{N_0}{2E_b})^{-1}, \tag{14}$$

$$E_b = \mathbf{E}_X[S], \qquad \mathrm{SIR} = \frac{E_b^2}{\sigma_{\mathrm{ISI}}^2 + \sigma_{\mathrm{MAI}}^2}, \tag{15}$$

where $Q(x)$ is the Marcum's Q-function, $\mathbf{E}_X[\cdot]$ denotes the expectation with respect to $\boldsymbol{X}$, and σ_{ISI}^2, and σ_{MAI}^2 are the variances of ISI and MAI, respectively. We evaluate the signal-to-interference ratio (SIR) of the receiver output.

4. Markov codes

Let $(X_0, X_1, \ldots, X_{N-1}) \in \{+1, -1\}^N$ be a sequence of binary random variables generated from an irreducible stationary Markov chain with transition probability matrix [20]

$$P = \frac{1}{2}\begin{pmatrix} 1+\lambda & 1-\lambda \\ 1-\lambda & 1+\lambda \end{pmatrix}, \quad (|\lambda| < 1). \tag{16}$$

Then we have $\mathbf{E}_X[X_n X_{n+\ell}] = \lambda^\ell$ $(\ell \geq 0)$.

Suppose that N and K are sufficiently large. Then, the SIR performance is evaluated by $E_b(\lambda)^2/\sigma_{\mathrm{MAI}}^2$. We obtain the energy per bit as

$$E_b(\lambda) = N \sum_{n=-\infty}^{\infty} \lambda^{|n|} \exp(-\{\pi\tau n\Delta f\}^2). \tag{17}$$

The variance of MAI is

$$\sigma_{\mathrm{MAI}}^2(\lambda) = N(K-1) \sum_{q=-\infty}^{\infty}\sum_{\ell=-\infty}^{\infty}\sum_{n=-\infty}^{\infty}\sum_{m=-\infty}^{\infty} \lambda^{|n|+|m|}$$
$$\cdot \exp\left(-\pi^2\tau^2((n-\ell)^2 + (m-\ell)^2)\Delta f^2 - \frac{q^2 T_d^2}{4\tau^2}\right). \tag{18}$$

Let $W_{tot} = 75$GHz and $N = 128$. Because of the lack of space, numerical results, such as optimum λ and optimum packing ratio in terms of SIR performance, are dropped but will be presented in the symposium.

References

[1] G. Mazzini, G. Setti, and R. Rovatti, "Chaotic complex spreading sequences for asynchronous DS-CDMA -part I: System modeling and results," *IEEE Trans. Circuits Syst. I*, vol. 44, no. 10, pp. 937–947, 1997.

[2] G. Mazzini, R.Rovatti, and G. Setti, "Interference minimisation by autocorrelation shaping in asynchronous DS/CDMA systems: Chaos based spreading is nearly optimal," *Electronics Letters, IEE*, vol. 35, pp. 1054–55, 1999.

[3] G. Setti, G. Mazzini, R. Rovatti, and S. Callegari, "Statistical modeling of discrete-time chaotic processes-basic finite-dimensional tools and applications," *Proc. IEEE*, vol. 90, no. 5, pp. 662 – 690, May 2002.

[4] G. Mazzini, G. Setti, and R. Rovatti, "Chip pulse shaping in asynchronous chaos-based DS-CDMA," *IEEE Trans. Circuits Syst. I*, vol. 54, no. 10, pp. 2299–2314, Oct. 2007.

[5] T. Kohda, "Information sources using chaotic dynamics," *Proc. IEEE*, vol. 90, no. 5, pp. 641–661, May 2002.

[6] S. Vitali, R. Rovatti, and G. Setti, "Improving PA efficiency by chaos-based spreading in multicarrier DS-CDMA systems," in *Proc. of ISCAS 2006*, 2006, pp. 1195–1198.

[7] G. Cimatti, R. Rovatti, and G. Setti, "Chaos-based spreading in DS-UWB sensor networks increases available bit rate," *IEEE Trans. on Circ. and Syst.-I*, vol. 54, no. 6, pp. 1327–1339, June 2007.

[8] ——, "Chaos-based generation of optimal spreading sequences for DS-UWB sensor networks," in *2006 Int. Sympo. Nonlinear Theory and Its Applications (NOTLA2006)*, Sept. 2006, pp. 583–586.

[9] L. Yang and G. B. Giannakis, "Ultra-wideband communications: An idea whose time has come," *IEEE Signal Processing Magazine*, pp. 26–54, Nov. 2004.

[10] B. Parr, B. Cho, K. Wallace, and Z. Ding, "A novel ultra-wideband pulse design algorithm," *IEEE Commun. Lett.*

[11] X. Wu, Z. Tian, T. N. Davidson, and G. B. Giannakis, "Optimal waveform design for UWB radios," *IEEE Trans. on Signal Processing*, vol. 54, no. 6, pp. 2009–2021, June 2006.

[12] A. Batra, J. Balakrishnan, G. R. Aiello, J. R. Foerster, and A. Dabak, "Design of a multiband OFDM system for realistic UWB channel environments," *IEEE Trans. on Microwave Theory and Techniques*, vol. 52, no. 9, Sept. 2004.

[13] A. D. Wyner, "The capacity of the band-limited Gaussian channel," *Bell Syst. Tech. J.*, vol. 45, pp. 359–395, Mar. 1966.

[14] D. Slepian and H. O. Pollak, "Prolate spheroidal wave functions, Fourier analysis, and uncertainty-I," *Bell Syst. Tech. J.*, vol. 40, no. 1, pp. 43–46, Jan. 1961.

[15] D. Slepian, "On bandwidth," *Proc. IEEE*, vol. 64, pp. 292–300, 1976.

[16] J. A. Morrison, "On the eigenfunctions corresponding to the bandpass kernel in the case of degeneracy," *Quart. Appl. Math.*, vol. 21, pp. 13–19, 1963.

[17] X. Luo, L. Yang, and G. B. Giannakis, "Designing optimal pulse-shapers for UWB radios," *J. Commun. Netw.*, vol. 5, no. 4, pp. 344–353, Dec. 2003.

[18] M. Z. Win and R. A. Scholtz, "Impulse radio: How it works," *IEEE Comm. Lett.*, vol. 2, no. 2, pp. 36–38, Feb. 1998.

[19] N. Boubacker and K. B. Lataief, "Performance analysis of DS-UWB multiple access under imperfect power control," *IEEE Trans. on Commun.*, vol. 52, no. 9, pp. 1459–1463, Sept. 2004.

[20] T. Kohda and H. Fujisaki, "Variances of multiple access interference: Code average against data average," *Electronics Letters, IEE*, vol. 36, pp. 1717–1719, 2000.